Mechanism-based constitutive modeling of $L1_2$ crystals

Y. Yuan*, D.M. Parks

Department of Mechanical Engineering, MIT, 77 Mass Ave. RM 1–321, Cambridge, MA 02139, USA

Abstract

A single-crystal constitutive model of the $L1_2$-structure intermetallic compound $Ni_3\,Al$ is developed, based on recent theoretical developments in dislocation mechanics and on experimental evidence. Hirsch's superkink-bypassing model and Caillard's self-unlocking mechanism have been modified and combined to describe dislocation dynamics in the yield anomaly region. Results of numerical simulations successfully capture major features of temperature dependence of the tensile yield strength and hardening rate over a range of crystallographic orientations.

Keywords: $L1_2$ crystals; Constitutive model; Dislocation mechanism; Superkink

1. Introduction

$L1_2$-structure compounds are well known for their anomalous mechanical behavior, typified by the positive temperature-dependence of yielding and hardening in certain temperature regions. In addition, these materials often exhibit orientation-dependent flow strength (non-Schmid behavior), and substantial flow strength reversibility in low/high/low temperature loading excursions. Since the first observations of the yield anomaly in $Ni_3\,Al$, intensive research has focused on discovering the underlying physical mechanisms responsible for these unusual mechanical behaviors, thus providing a mechanistically informed basis for constitutive modeling.

Based on the cross-slip-induced point-obstacle model [1] prevalent in the 1980s, Cuitino and Ortiz [2] proposed a constitutive model for $L1_2$ crystals which invoked forest-type hardening. They took the yield anomaly as a manifestation of hardening, since anomalous yielding is observed only for small offset strains. Explicit expressions for the hardening rate of cube and octahedral slip systems were developed, both having the form:

$$\dot{\gamma}^{\alpha} = \begin{cases} \dot{\gamma}_0{}^{\alpha}[(\tau^{\alpha}/g^{\alpha})^{1/m} - 1] & (\text{if } \tau^{\alpha} > g^{\alpha}) \\ 0 & (\text{otherwise}) \end{cases}$$

where m is the strain-rate sensitivity exponent, $\dot{\gamma}_0{}^{\alpha}$ is a reference shear strain-rate, τ^{α} is the resolved shear stress, and g^{α} is the resistance.

The evolution equation for g^{α} was based on an assumed point-obstacle density. For cube systems, changes in obstacle density were assumed due only to forest dislocation multiplication, while for octahedral systems, PPV-type-cross-slip-induced pinning [1] was also accounted for. Since the density of the latter point obstacles should increase with increasing temperature, due to thermally activated cross-slip, an anomalous temperature-dependence of flow strength is expected. Numerical simulation results based on this constitutive model, which captured major features of anomalous yielding in $L1_2$ crystals, were also presented.

However, based on subsequent TEM observations and dislocation modeling, it is now widely accepted [3,4,5,6,7], that the obstacles hindering movement of screw dislocations on the octahedral planes are actually long sessile screw segments locked in the Kear-Wilsdorf (K-W) configuration, rather than mere 'point obstacles'. The extremely high hardening rate (up to 40% of shear modulus) and the noted flow strength reversibility also counterindicate forest-type hardening as the dominant mechanism. Here, we develop a new single-crystal constitutive model, based on recent theoretical developments, which can capture the anomalous temperature dependence in both yielding and hardening for $L1_2$ crystals.

* Corresponding author. Tel.: +1 617 253 5353;
E-mail: yiny@mit.edu

Computational Fluid and Solid Mechanics 2005
K.J. Bathe (Editor)

2. General constitutive framework

Major equations of the single-crystal plasticity constitutive framework were described by Kalidindi, et al. [8]. The plastic flow rate, L^P, is comprised of the superposition over the active slip systems, α, of the crystallographic plastic shear rates ($L^P = \sum \gamma^\alpha \, \mathbf{m}_0^\alpha \otimes \mathbf{n}_0^\alpha$), where $\mathbf{m}_0^\alpha$ and $\mathbf{n}_0^\alpha$ are unit lattice vectors $^\alpha$denoting slip direction and slip plane normal, respectively. The plastic shearing strain rate on each system, $\dot{\gamma}^\alpha$, is given by Orowan's equation, $\dot{\gamma}^\alpha = \rho_{\mathrm{m}}^\alpha b \bar{v}^\alpha$, which provides a connection between macro-deformation and the micro-dislocation-dynamics. Here $\rho^\alpha{}_{\mathrm{m}}$ is the density of mobile dislocations for slip system α, b is the magnitude of the Burgers vector, and $\bar{v}^\alpha$ is the average dislocation velocity.

3. Dislocation mechanics

Among the numerous models attempting to explain dislocation dynamics $L1_2$ in crystals, Hirsch's superkink model [3] and Caillard's self-unlocking model [4] are most prominent. In Hirsch's model, flow on an octahedral slip system was simplified, represented by a single screw dislocation having equally separated superkinks of a common height. Unlocking was assumed to be rate-controlling and due to the bypassing of superkinks along the locked screw segments. The resulting average dislocation velocity was given by $\bar{v} = v_f \exp[-(H_u - H_l)/kT]$, where ν_f is the free-flight velocity, H_l is essentially the PPV-type locking enthalpy, which involves non-Schmid stress components so that the orientation-dependent feature of the yield anomaly can be well-modeled, and H_u is the unlocking activation enthalpy, given as $H_u = H_{u0} - V(l)\,\tau$. Here, H_{u0} is a constant ($\sim$2 ev), and V is the activation volume, proportional to the superkink height, l.

Caillard's self-unlocking mechanism was based on his *in situ* TEM observations of the jerky movements of screw dislocations. Flow strength was identified with a critical octahedral stress, above which the cross-slip driving force on the trailing superpartial dislocation would exceed that on the leading one, so that K-W locks could be unlocked by preferential cross-slipping of the trailing superpartial. Flow strength (critical applied octahedral shear stress τ) was derived as a function of cross-slipped distance w, and material variables including fault energies and the elastic anisotropy factor. Yielding anomalies were explained as the strengthening of K-W locks, due to increasing cross-slip distance w, with increasing temperature.

These two unlocking mechanisms are modified, combined, and implemented in the proposed constitutive model. For each octahedral slip plane, we assume that the superkinks' population shows an exponential form distribution over its height, $f_1(l) = C_0 \exp(-l/l_o)$, as observed by Couret et al. [9]. Here, l represents superkink's height, and and C_0 and l_o are temperature-related parameters governing the distribution. Since the activation volume in the superkink unlocking mechanism is proportional to l, longer superkinks are easier to activate, and the mobility of a screw segment is determined by the height of its superkinks. The plastic strain rate of each octahedral slip system achieved via the superkink bypassing mechanism is defined by:

$$\dot{\gamma}_{(1)}{}^\alpha = b v_f \rho_{total}^\alpha \int_0^{l_{\max}^\alpha} f_1(l^\alpha) \exp\left(-\frac{H_u(l^\alpha, \tau^\alpha) - H_l}{kT}\right) dl^\alpha \quad (\alpha = 1 - 12) \tag{1}$$

Because the activation volume V is large ($\sim 100b^3$), the integral of Eq. (1) is dominated by its upper limit, $l_{\max}$. Under a given stress, K-W locks are unlocked by the relatively few longest superkinks, while the more numerous shorter ones hardly have a chance to be activated. When unlocked screws relock after advancing, the newly generated superkinks obey the same exponential form distribution and are mostly very short. Previously mobile screws become sessile, and, to sustain flow, stress must be increased in order to activate screws with the 'next-longest' superkinks. Thus, the hardening rate is closely related with the evolution of $l_{\max}$, which is modeled as:

$$\dot{l}_{\max} = \frac{dl_{\max}}{dt} = \frac{dl_{\max}\dot{\gamma}}{d\gamma} \approx \frac{\Delta l_{\max}\dot{\gamma}}{\Delta \rho b l_{\max}} \approx \frac{-\dot{\gamma}}{f_1(l_{\max})\rho_{total} b l_{\max}} \tag{2}$$

At the high-temperature end of the yield anomaly region, when the applied octahedral shear stress exceeds a critical value, $\tau_{critical}$, locked screw segments lacking mobile superkinks can be unlocked by the self-unlocking mechanism. $\tau_{critical}$ is derived in a way similar to Caillard's derivation of flow stress, as a function of w and material variables. The octahedral system plastic strain rate achieved by this mechanism is given by:

$$\dot{\gamma}_{(2)}{}^\alpha = b \rho_{total}^\alpha \int_0^{w_{\max}} f_2(w) v_{(2)}{}^\alpha(w,\tau) dw \quad (\alpha = 1 - 12) \tag{3}$$

where $f_2(w)$ is assumed to be a normal distribution of w, centered at $\bar{w}(T)$, an increasing function of temperature. $\nu_{(2)}{}^\alpha$ is the average dislocation velocity corresponding to the self-unlocking mechanism, defined as:

$$v_{(2)}{}^\alpha = v_f\left[\left(\frac{\tau^\alpha}{\tau_{critical}}\right)^{m_1} - 1\right] \quad \text{If } \tau^\alpha > \tau_{critical}; \quad v^\alpha = 0 \quad \text{otherwise;} \tag{4}$$

where m_1 is a rate sensitivity exponent. The total plastic strain rate for the octahedral systems, $\dot{\gamma}^{\alpha}$, is the summation of Eqs. (1) and (3): $\dot{\gamma}^{\alpha} = \dot{\gamma}_{(1)}{}^{\alpha} + \dot{\gamma}_{(2)}{}^{\alpha}$, $(\alpha = 1 - 12)$.

For cube slip, $\dot{\gamma}^{\alpha}$ is represented by standard power-law form, $\dot{\gamma}^{\alpha} = \dot{\gamma}_{o}(\tau^{\alpha}/s^{\alpha})^{m_2}$, $\alpha = (13 - 18)$. The evolution of cube resistance, s^{α}, is given by $\dot{s}^{\alpha}/s^{\alpha} = C_2\dot{\gamma}^{\alpha}$, with an initial value s_o^{α} linearly decreasing with temperature. Here, $\dot{\gamma}_o$, m_2 and C_2 are constants.

4. Simulation results and discussion

The proposed constitutive model is implemented into a simple Matlab solver and a finite element solver, both with implicit algorithms. Simulations of uniaxial-tension of single crystals under an applied strain-rate of 10^{-4}/s for the three corner orientations of the spherical triangle have been applied. Simulated stress-strain curves for (111) and (001) orientations at different temperatures are shown in Figs. (1) and (2), respectively. The temperature-dependence of 0.1% tensile yield strength and tensile hardening modulus, $\bar{h}$, for all three orientation, are illustrated in Figs. (3) and (4).

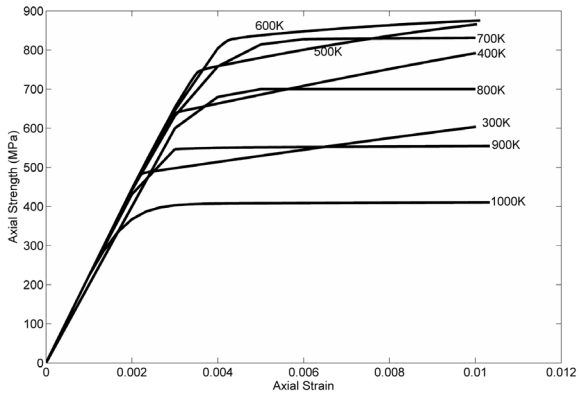

Fig. 1. Simulated uniaxial stress-strain curves for (111) orientation at different temperatures.

Simulation results successfully capture major features of the temperature-dependence of yield strength and $\bar{h}$: they both increase with increasing temperature for all orientations until the respective peak temperatures $T_{p,\tau}$ and $T_{p,h}$. The magnitude of $T_{p,h}$ is smaller than that of $T_{p,\tau}$, as experimentally observed. Orientation-dependence of $T_{p,\tau}$ is due to the different Schmid factors of cube planes for these orientations: largest in (111), zero in (001). Decreases of $\bar{h}$ for (001) and (011) orientations

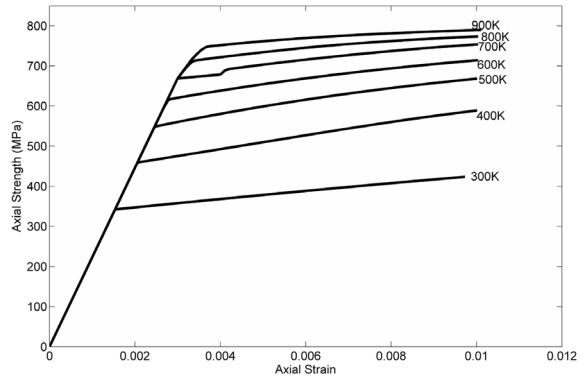

Fig. 2. Simulated uniaxial stress-strain curves for (001) orientation at different temperatures.

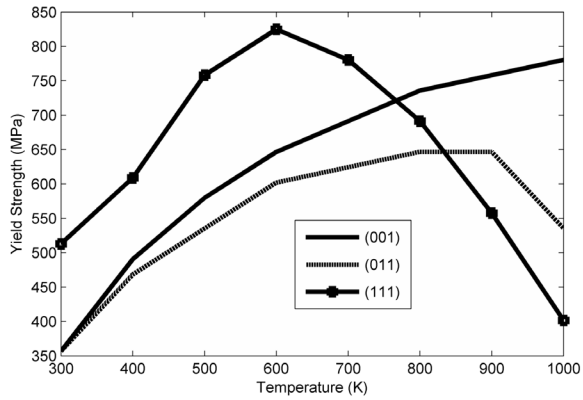

Fig. 3. Temperature dependence of 0.1% yield strength for different orientations.

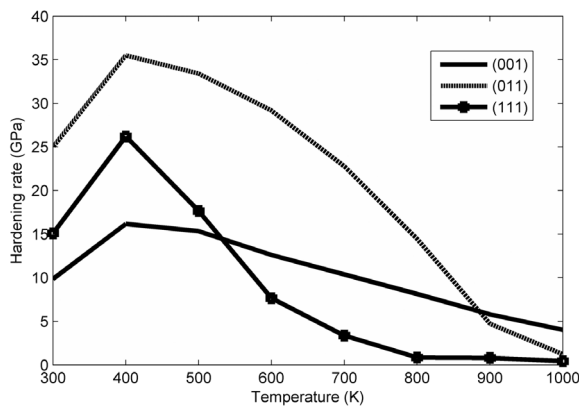

Fig. 4. Temperature dependence of hardening rate for different orientations.

are due to activation of the self-unlocking mechanism at high temperature (and high stress). For the (111) orientation, decreases of $\bar{h}$ are also partially due to the activation of cube slip, consistent with observations of Lall et al. [10], that cube slip is activated for orientations close to (111) at temperatures lower than $T_{p,\tau}$.

5. Summary

A constitutive model has been developed based on the superkink-bypassing mechanism and the self-unlocking mechanism. Simulation results capture the major features of the temperature-dependence of both yield strength and hardening modulus. In future study, fault energy related orientation dependence and composition effects of yielding and hardening should be considered in more detail.

Acknowledgment

This research was supported in part through the DARPA AIM initiative, subcontracted through United Technologies under contract DE-FC36-04G014040 to MIT.

References

[1] Paidar B, Pope DP, Vitek V. Acta Metall Mater 1984; 32(3):435–448.
[2] Cuitino AM, Ortiz M. Mater Sci Eng 1992;170:111–123.
[3] Hirsch PB. Phil Mag A 1992;65(3):569–612.
[4] Caillard D, Paidar V. Acta Mater 1995;44, No. 7:2759–2771.
[5] Louchet F. Journal de Physique III 1995;5:1803–1807.
[6] Veyssiere P, Saada G. Dislocations in Solids 1996;10:265–441.
[7] Viguier B, Martin JL, Bonneville J. Dislocations in Solids 2002;11:459–545.
[8] Kalidindi SR, Bronkhorst CA, Anand L. J Mech Phys Solids 1992;40:537–569.
[9] Couret A, Sun YQ, Hirsch PB. Phil Mag A 1992;67, No. 1:29–50.
[10] Lall C, Chin S, Pope DP. Metall Trans 1979;10A:1323–1332.